

Rectified quantized charging of gold nanoparticle self-assembled monolayers by arenedithiol linkages

Shaowei Chen* and Fengjun Deng

Department of Chemistry, Southern Illinois University, Carbondale, Illinois 62901

ABSTRACT

Gold nanoparticle self-assembled monolayers were fabricated by a sequential anchoring mechanism with rigid arenedithiol chemical linkers. These particle surface assemblies exhibited well-defined quantized capacitance characters in aqueous solutions, and more importantly, in aqueous solutions, the voltammetric responses were rectified in the presence of hydrophobic anions, which was interpreted on the basis of a Randle's equivalent circuit where the particle-ion pairing formation led to the manipulation of electrode interfacial double-layer capacitance. The effective nanoparticle capacitances evaluated from the voltammetric measurements were consistent with those with the particles immobilized onto electrode surfaces by alkanedithiols. In addition, the nanoparticle electron-transfer kinetics was investigated by AC voltammetry and the rate constants were generally found of the order of 10^3 s^{-1} , at least an order of magnitude greater than those with saturated alkyl spacers.

KEYWORDS: Rectification, electron transfer, quantized charging, nanoparticle, arenedithiol, self-assembled monolayer

1. INTRODUCTION

Recently, we discovered that the quantized capacitance charging of monolayer-protected gold nanoparticles (Au MPCs) could be rectified by hydrophobic ions in aqueous solutions when the particles were immobilized onto electrode surfaces forming long-range ordered assemblies.¹ These unique charge-transfer behaviors were interpreted on the basis of a Randle's equivalent circuit. In this model circuit, the electrode interfacial double-layer capacitance is comprised of two parts, C_{SAM} for the collective contributions of all surface-anchored nanoparticle molecules, and C_{DL} for the electrode surface that is not covered by nanoparticles (i.e., the so-called interparticle void space). It has been found that in low-dielectric organic media discrete chargings to the particle nanoscale molecular capacitance were very well-defined at potentials both positive and negative of the potential of zero charge (PZC). However, in aqueous solutions, the quantized capacitance charging features were only observed in the presence of hydrophobic electrolyte anions (e.g., PF_6^- , ClO_4^- , and BF_4^-) and at potentials more positive than the PZC, leading to a voltammetric current that is substantially larger than that in the negative potential regime (viz., rectified quantized charging). This is ascribed to the effects of MPC-ion pair formation where the adsorption of hydrophobic anions expels the water molecules from the interface, resulting in $C_{\text{SAM}} > C_{\text{DL}}$ and hence the overall voltammetric currents were mainly due to the quantized charging through the nanoparticle molecular capacitance. This is in sharp contrast to the case in organic media where generally $C_{\text{SAM}} > C_{\text{DL}}$ in all potentials thus the quantized charging characters can be observed at potentials both positive and negative of PZC. These earlier studies indicate that nanoscale electron transfers can be readily manipulated by simple ion chemistry.

In contrast, in the presence of "hard" electrolyte anions (e.g., NO_3^- , PO_4^{3-} , and SO_4^{2-}), the nanoparticle surface assemblies exhibit voltammetric responses akin to those for a conventional molecular diode with only featureless current profiles.¹ Therefore, one can see that a transition from conventional molecular diode to single-electron rectifier can be effected by increasing the "softness" of the electrolyte ions. Additionally, the onset potential has been found to be sensitive to the softness of the electrolyte ions as well, shifting cathodically (anodically) with increasing hydrophobicity of anions (cations). This provides a mechanistic basis for the regulation of nanoscale electron transfers.

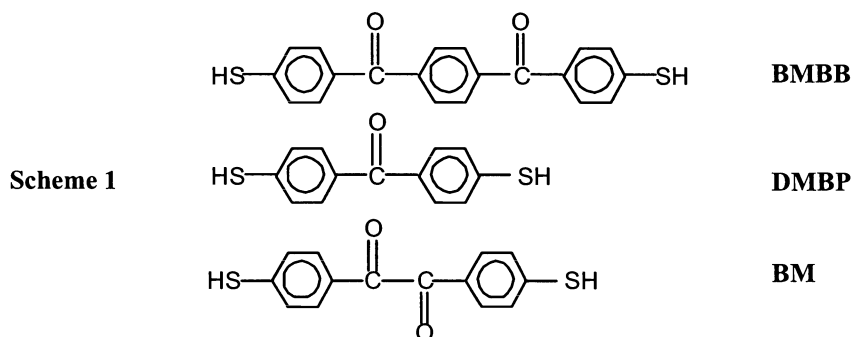
* To whom all correspondence should be addressed. E-mail: schen@chem.siu.edu

Furthermore, the electron transfer kinetics of nanoparticle quantized charging was examined by using AC voltammetry as well as electrochemical impedance spectroscopy.^{1,2} The rate constants were found to be of the order of $10 - 100 \text{ s}^{-1}$ and decreased exponentially with increasing alkyl spacers, indicating a tunneling mechanism for the charge-transfer processes. Additionally, the tunneling coefficient (β) was estimated to be 0.8 \AA^{-1} which is very close to that obtained in solid-state electronic conductivity measurements using nanoparticle dropcast thick films,³ as well as in consistence with the typical values found with ω -tethered two-dimensional self-assembled monolayers (SAMs).⁴ However, thus far the effects of aryl spacers on the nanoparticle charge-transfer chemistry have not been probed. It is anticipated that the introduction of unsaturated spacers will facilitate electron transfer, akin to that observed previously⁵ with conventional SAMs with ω -functionalized redox-active moieties. Thus, in this paper, we first immobilized gold nanoparticles onto electrode surfaces with rigid arenedithiol chemical linkers by using a sequential anchoring method, and investigated their unique rectified quantized charging in aqueous solutions. The associated electron-transfer kinetics was found to be at least an order of magnitude faster than that found with alkyl spacers of similar length.

2. EXPERIMENTAL SECTION

Chemicals. Potassium hexafluorophosphate (KPF_6 , 99%, ACROS), n-pentanethiol (C_5SH , 98%), n-hexanethiol (C_6SH , 96%), n-heptanethiol (C_7SH , 95%), n-octanethiol (C_8SH , 97%), n-nondecaneithiol (C_9SH , 95%) and n-decanethiol (C_{10}SH , 96%) were all used as received from ACROS. All solvents were obtained from typical commercial sources and used as received as well. Water was supplied by a Barnstead Nanopure water system ($18.3 \text{ M}\Omega$).

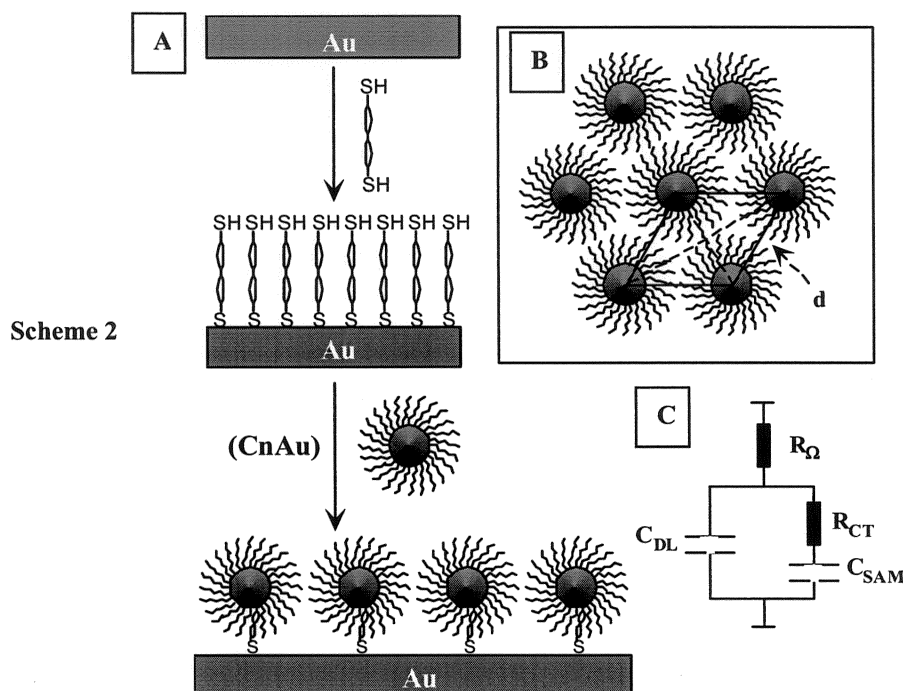
Three arenedithiols (Scheme 1), 1,3-Bis(4-mercaptobenzoyl)benzene (BMBB), 4,4'-Dimercaptobenzophenone (DMBP) and 4,4'-mercaptobenzil (BM), were synthesized and characterized by following a literature protocol.⁶



Synthesis of gold nanoparticles. Alkanethiolate monolayer-protected gold (C_nAu) nanoparticles were prepared by using the Schiffrin route,⁷ which were denoted as C_nAu with C_n referring to the corresponding alkanethiolate ligands. The particles were first fractionated by using a solvent and nonsolvent mixture (e.g., toluene and ethanol) to narrow the size dispersity, and then thermally annealed by refluxing in toluene for 4 to 8 hrs.⁸ The resulting particles were found to be highly monodisperse in core size and shape (spherical) with the core diameter of $\sim 2.0 \text{ nm}$ and less than 10% dispersity (determined by transmission electron microscopic measurements).

Self-assembly of gold nanoparticles. The nanoparticles were assembled onto the electrode surface by using a sequential anchoring route⁹ (Scheme 2). Experimentally, a gold electrode was first polished with $0.05 \mu\text{m}$ Al_2O_3 slurries and rinsed with copious dilute HNO_3 , H_2SO_4 , and Nanopure water successively. The electrode was then subject to electrochemical etching by rapid potential sweep (10 V/s) for 5 min in 0.10 M H_2SO_4 within the potential range of $+1.2$ and -0.2 V . The cleaned electrode was then incubated into an N,N -dimethylformide (DMF) solution of one of the arenedithiols (1 mM) for 1 day. The electrode was rinsed with copious DMF to remove loosely bound dithiol ligands and dried in a gentle nitrogen stream before being immersed into a hexane solution of C_nAu particles (3 mg/mL) for 7~14 days. Longer exposure time did not seem to result in substantial improvement of the nanoparticle surface coverage though the details of the adsorption dynamics was not investigated. Finally, the electrode was rinsed with hexane and dried again in a nitrogen stream prior to being introduced into an electrolyte solution for electrochemical measurements.

Electrochemical Studies. Electrochemical measurements were carried out with a BAS 100BW or CHI440 Electrochemical Workstation. The gold electrode with the nanoparticle adsorbed monolayers was used as the working electrode, a Ag/AgCl (3 M NaCl, from BAS) and a Pt coil were used as the reference and counter electrodes, respectively. The solutions were deaerated for at least 20 min prior to data acquisition by high-purity nitrogen which was saturated by water and blanketed with an atmosphere of N₂ during the entire experimental procedure.



3. RESULTS AND DISCUSSION

The surface-anchored gold nanoparticle assemblies exhibit well-defined quantized capacitance charging features. Figure 1 shows some representative cyclic (CVs, panels A, C, and E) and differential pulse voltammograms (DPVs, panels B, D, and F) for C6Au particles linked to the electrode surface by the three different arenedithiol ligands (Scheme 1) in 0.1 M KPF₆. Similar responses were also observed with other gold nanoparticles (e.g., from C4Au to C10Au). One can see that overall the current responses are similar to those observed when the particles were immobilized onto the electrode surfaces by alkanedithiol chemical bridges or metal ion chelation.¹ At $E > -0.2$ V, the currents show a series of well-defined voltammetric peaks which are ascribed to the quantized charging to the surface-immobilized nanoparticle capacitance whereas at $E < -0.2$ V, the current responses are essentially featureless. Furthermore, one can see that the currents at $E > -0.2$ V are substantially larger than that at $E < -0.2$ V. Again, these rectifying characters are accounted for by the binding of hydrophobic anions (PF₆⁻) to the nanoparticle molecules, leading to the manipulation of interfacial double-layer capacitance (Scheme 2 C). This ion-pairing mechanism has also been used to account for the variation of onset potentials (E_{on}) of the rectification with electrolyte composition,¹ where it has been found previously that E_{on} exhibits a cathodic (anodic) shift with increasing hydrophobicity of the anions (cations), akin to the effects of specific adsorption on electrode potential of zero charge.

As these voltammetric peaks represent successive $1e^-$ chargings to the nanoparticle molecular capacitance (C_{MPC}), the corresponding formal potentials ($E^{o'}$) have been found to be related to the particle charge state (z),¹⁰

$$E_{z,z-1}^{o'} = E_{PZC} + \frac{(z-\frac{1}{2})e}{C_{MPC}} \quad (1)$$

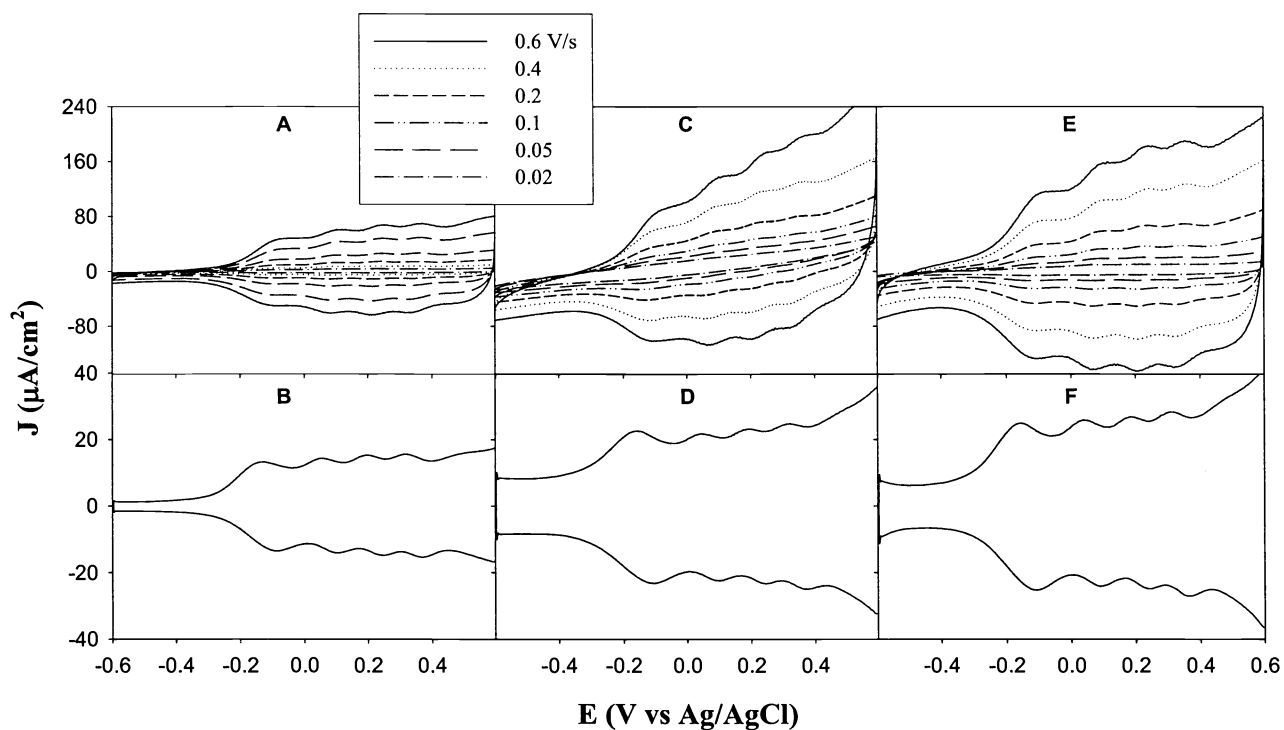


Figure 1 Cyclic (CV, panels A, C, and E) and differential pulse voltammograms (DPV, panels B, D, and F) of C6Au nanoparticles anchored onto a gold electrode surface via varied arenedithiol linkages in 0.1 M KPF₆: panels A and B, BMBB; panels C and D, DMBP; panels E and F, BM. Electrode area 1.9 mm². In CV, potential scan rates shown in figure legends; and in DPV, DC ramp 20 mV/s, pulse amplitude 50 mV.

where E_{PZC} is the particle potential of zero charge, and e is the electronic charge. Figure 2 shows the variation of the formal potentials of C6Au charging peaks with the particle charge states. One can see that the relationship is linear as anticipated from Eq. (1) with all three arenedithiol linkers. From the slopes and intercepts of the linear profiles of $E^{0'}$ vs z , one can then evaluate C_{MPC} as well as E_{PZC} . The results are summarized in Table 1. One can see that the nanoparticle molecular capacitance is generally around 1 aF and decreases with increasing chainlengths of the protecting alkanethiolates. The particle capacitance is also found to be virtually invariant of the arenedithiol linkers, indicating that the dielectric properties of the protecting monolayers remain essentially unchanged despite the fact that during the anchoring process multiple copies of arenedithiol linkers replace the original alkanethiolates adsorbed on the particle surfaces. In addition, the capacitances are generally comparable to those with particle assemblies linked by alkanedithiols.¹ In comparison to the results where the electrochemical measurements were carried out in organic media, the nanoparticle capacitances in aqueous solutions were significantly larger.¹

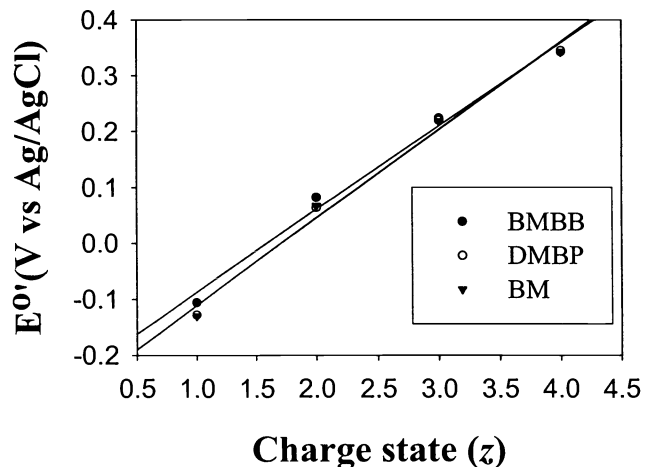
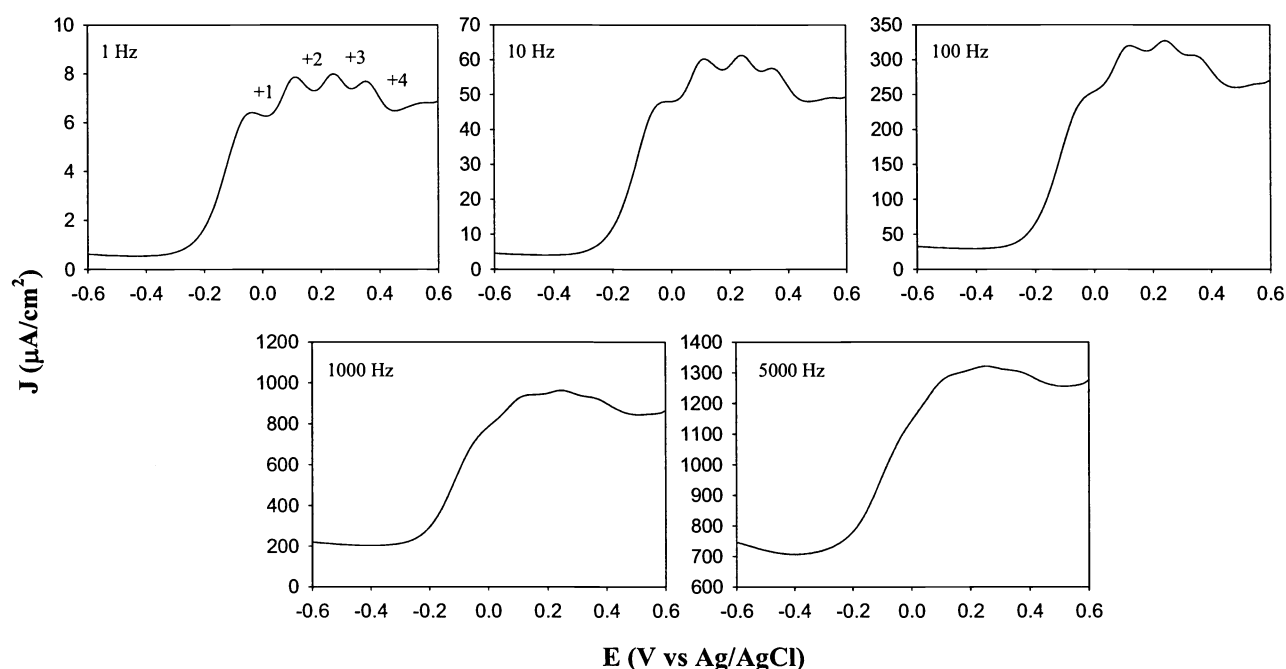


Figure 2 Variation of the formal potentials of C6Au quantized chargings with particle charge state. Symbols are experimental data obtained from the DPV measurements in Figure 1 and lines are the corresponding linear regressions.

Table 1 Effective nanoparticle molecular capacitance and electron transfer rate constants with varied arenedithiol linkers

	BMBB		DMBP		BM	
	C_{MPC} (aF)	k_{ET} (s^{-1}) [¶]	C_{MPC} (aF)	k_{ET} (s^{-1}) [¶]	C_{MPC} (aF)	k_{ET} (s^{-1}) [¶]
C5Au	1.18	2215 ± 597				
C6Au	1.08	898.1 ± 163.8	1.02	2190.4 ± 397.7	1.02	3143.5 ± 287.1
C7Au	1.08	1097.8 ± 396.6				
C8Au	1.05	129.8 ± 20.0				
C9Au	0.98	547.2 ± 132.7				
C10Au	0.89	801.7 ± 40.7				

¶average of the values at various nanoparticle charge states

**Figure 3** AC voltammograms (ACV) of C6Au nanoparticles immobilized onto a gold electrode surface by BMBB self-assembled monolayers (Figure 1) at varied frequencies (shown as figure legends).

The electron-transfer kinetics of these quantized charging processes was then evaluated by using AC voltammetry (ACV).^{1b,2} The MPC quantized charging represents a novel electrochemical redox phenomenon, whose electron-transfer chemistry remains largely unexplored. Previously we used two electrochemical techniques to probe the kinetic aspects of these unique electron-transfer processes, one based on the Laviron method and the other based on AC voltammetry (or impedance spectroscopy).^{1,2} Both methods yielded a rather consistent rate constant. The unique advantage of ACV technique is that for surface-immobilized redox-active systems, by varying the AC frequency, one can manipulate the current contributions from the faradaic as well as background (double-layer charging) components. Thus, for nanoparticle surface assemblies, at low frequencies, the quantized charging features are very well-defined and the currents are much larger than that of the background; whereas at high frequencies, the electron-transfer processes are not fast enough to catch up with the AC perturbation and hence the overall current response is reduced to that of the background. Figure 3 depicts the AC voltammograms of C6Au anchored onto a self-assembled monolayer of BMBB at varied AC frequencies. One can see that with increasing AC frequencies, the discrete charging peaks become less well-defined and while both the peak currents (I_p) and background contributions (I_b) increase with frequency, the ratio of I_p/I_b decreases with frequency and approaches unity at high frequency (Figure 4).

By fitting the experimental data with the Randle's equivalent circuit (Scheme 2C), one can evaluate the charge-transfer resistance (R_{CT}) as well as the collective contributions of all surface-anchored nanoparticle molecular capacitance (C_{SAM}). From these, one can then estimate the electron-transfer rate constants by the following equation,

$$k_{ET} = \frac{1}{2R_{CT}C_{SAM}} \quad (2)$$

The results are summarized in Table 1. First, one can see that in general, the electron-transfer rate constants are of the order of 10^2 to 10^3 s^{-1} , at least an order of magnitude larger than those with nanoparticle ensembles anchored by alkyl spacers despite much longer chainlength of these aryl linkers (the chainlengths of these chemical linkers as calculated by Hyperchem[®] are: BMBB, 1.69 nm; DMBP, 1.14 nm; BM, 1.31 nm; C6SH, 0.78 nm).¹ Second, the electron-transfer rate constants increase with decreasing chainlengths of the aryl spacers (e.g., C6Au). These observations can be interpreted by the aromatic nature of the electron-transfer barriers, as observed previously with self-assembled monolayers with ω -functionalized conventional redox moieties.⁵

It should be noted that for a specific nanoparticle monolayer anchored by one of the arenedithiols the rate constants do not appear to depend on the particle charge state, a behavior similar to previous observations where the nanoparticles are self-assembled by alkanedithiol chemical bridges.¹ Thus data shown in Table 1 are the average over several charge states. In addition, one might also notice that even with the same arenedithiol linkers, the electron-transfer rate constants fluctuate somewhat with nanoparticle chemical structures (e.g., protecting monolayers). For instance, one can see from Table 1 that with BMBB linkers, the rate constant decreases somewhat from C5Au to C8Au and then increases slightly. Since the particle core dimension is very similar among these different particles, the observed discrepancy in electron-transfer rate constants might be attributable to the difference in nanoparticle monolayer structures reflected, for instance, in the interactions of the arenedithiol ligands with the particle protecting monolayers (e.g., number of anchoring sites). Further studies are desired to investigate the surface structures of the nanoparticle assemblies to provide more insight into the relationship between the nanoscale chemical environments and electron-transfer chemistry.

One might note that overall the rate constants evaluated from nanoparticle surface organized assemblies are a few orders of magnitude smaller than those obtained from solid-state conductivity measurements with nanoparticle dropcast thick films³ or voltammetric studies with nanoparticle surface multilayers by metal ion complexation¹¹ where the rate constants for electron hopping between neighboring particles were found to be of the order of 10^6 s^{-1} . While the details remain to be explored, the difference might originate from the interaction of hydrophobic anions with nanoparticle molecules in aqueous solutions. It has been found that for viologen self-assembled monolayers supported onto electrode surfaces, the ion-pair formation between viologen moieties and hydrophobic electrolyte anions slows down quite significantly the electron-transfer kinetics of viologen redox processes, where the viologen voltammetric currents diminish with increasing concentration of PF_6^- .¹² Such an ion-pair effect is suspected to account for the observed small rate constants of nanoparticle charge-transfer chemistry. More studies are currently underway to investigate the effects of electrolyte composition on nanoscale charge-transfer dynamics.

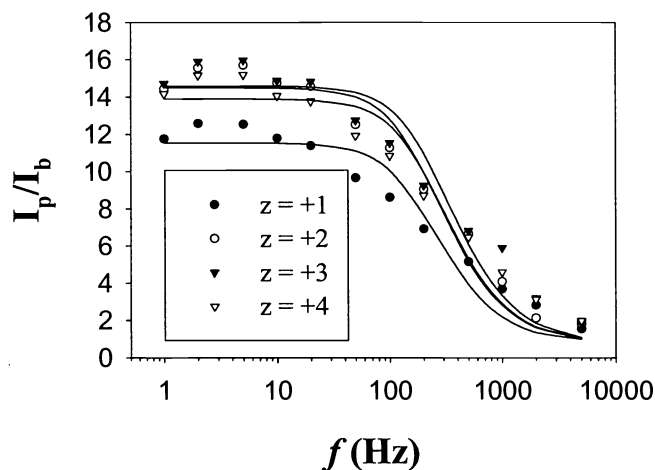


Figure 4 Variation of the ratios of charging peak currents to background currents with AC frequencies at different charge states of the particles. Symbols are experimental data obtained from Figure 3 and lines are fits by the Randle's equivalent circuit in Scheme 2 C.

4. CONCLUDING REMARKS

Gold nanoparticle surface organized assemblies were fabricated by using a sequential anchoring mechanism with arene-dithiol monolayers. The resulting particle monolayers exhibited well-defined quantized capacitance charging features which were rectified in the presence of hydrophobic electrolyte anions. The ion-induced rectification was interpreted on the basis of a Randle's equivalent circuit. Electron-transfer kinetics was investigated by AC voltammetry and the rate constants were found to be of the order of 10^2 to 10^3 s⁻¹ for these three arene-dithiols, and at least an order of magnitude larger than those with saturated alkyl chemical linkers. This was ascribed to the aromatic nature of these aryl spacers which facilitated electron transfer between the particles and the electrode.

ACKNOWLEDGMENTS

The authors are grateful to Ms. Junge Lu for the assistance in the synthesis of the arene-dithiol ligands. This work was supported, in part, by the National Science Foundation (CAREER Award), the ACS Petroleum Research Fund, and the SIU Materials Technology Center. S. C. is a Cottrell Scholar of Research Corporation.

REFERENCES

1. (a) S. Chen, "Nanoparticle assemblies: 'rectified' quantized charging in aqueous media", *J. Am. Chem. Soc.* **122**, 7420-7421, 2000. (b) S. Chen, R. Pei, "Ion-Induced rectification of nanoparticle quantized charging in aqueous media", *J. Am. Chem. Soc.* **123**, 10607-10615, 2001. (c) S. Chen, R. Pei, T. Zhao, D. J. Dyer, "Nanoparticle assemblies based on metal ion:pyridine chelation and their rectified quantized charging in aqueous solutions", *J. Phys. Chem. B* **106**, 1903-1908, 2002.
2. S. Chen, "Self-Assembling of Monolayer-Protected Gold Nanoparticles", *J. Phys. Chem. B* **104**, 663-667, 2000.
3. W. P. Wuelfing, S. J. Green, J. J. Pietron, D. E. Cliffler, R. W. Murray, "Electronic conductivity of solid-state, mixed-valent, monolayer-protected Au clusters", *J. Am. Chem. Soc.* **122**, 11465-11472, 2000.
4. (a) C. E. D. Chidsey, C. R. Bertozzi, T. M. Putvinski, A. M. Majsce, "Coadsorption of ferrocene-terminated and unsubstituted alkanethiols on gold: electroactive self-assembled monolayers", *J. Am. Chem. Soc.* **112**, 4301, 1990. (b) S. E. Creager, G. K. Rowe, "Solvent and double-layer effects on redox reactions in self-assembled monolayers of ferrocenyl-alkanethiolates on gold", *J. Electroanal. Chem.* **420**, 291-299, 1997.
5. S. E. Creager, C. J. Yu, C. Bambad, S. O'Connor, T. MacLean, E. Lam, Y. Chong, G. T. Olsen, J. Luo, M. Gozin, L. F. Kayyen, "Electron transfer at electrodes through conjugated 'molecular wires' bridges", *J. Am. Chem. Soc.* **121**, 1059-1064, 1999.
6. Y. Ding, A. S. Hay, "Cyclic aromatic disulfide oligomers: synthesis and characterization", *Macromolecules* **29**, 6386-6392, 1996.
7. (a) M. Brust, M. Walker, D. Bethel, D. J. Schiffrin, R. Whyman, "Synthesis of thiol-derivatised gold nanoparticles in a two-phase liquid-liquid system", *J. Chem. Soc. Chem. Comm.* 801-802, 1994. (b) A. C. Templeton, W. P. Wuelfing, R. W. Murray, "Monolayer-protected Cluster Molecules", *Acc. Chem. Res.* **33**, 27-36, 2000. (c) R. L. Whetten, M. N. Shafiqullin, J. T. Khoury, T. G. Schaaff, I. Vezmar, M. M. Alvarez, A. Wilkinson, "Crystal Structures of Molecular Gold Nanocrystal Arrays", *Acc. Chem. Res.* **32**, 397-406, 1999.
8. (a) M. M. Maye, W. Zheng, F. L. Leibowitz, N. K. Ly, C.-J. Zhong, "Heating-induced evolution of thiolate-encapsulated gold nanoparticles: a strategy for size and shape manipulations", *Langmuir* **16**, 490-497, 2000. (b) S. Chen, "Langmuir-Blodgett fabrication of two-dimensional robust crosslinked nanoparticle networks", *Langmuir* **17**, 2878-2884, 2001.
9. S. Chen, R. W. Murray, "Electrochemical quantized capacitance charging of surface ensembles of nanoparticles", *J. Phys. Chem. B* **103**, 9996-10000, 1999.
10. S. Chen, R. W. Murray, S. W. Feldberg, "Quantized capacitance charging of monolayer-protected Au clusters", *J. Phys. Chem. B* **102**, 9898-9907, 1998.
11. J. F. Hicks, F. P. Zamborini, A. J. Osisek, R. W. Murray, "The dynamics of electron self-exchange between nanoparticles", *J. Am. Chem. Soc.* **123**, 7048-7053, 2001.
12. S. Chen, F. Deng, unpublished results.